ELSEVIER

Thermochimica Acta 361 (2000) 53–60

thermochimica acta

www.elsevier.com/locate/tca

Two oxidation states and four different coordinations of iron in an unusual chloro complex TG–MS, Raman and Mössbauer spectroscopic investigations of the thermal behaviour

M. Feist[a], R. Kunze[b], D. Neubert[b], K. Witke[b], H. Mehner[b], E. Kemnitz[a,*]

[a]*Institute of Chemistry, Humboldt University, Hessische Strasse 1-2, D-10115 Berlin, Germany*
[b]*Bundesanstalt für Materialforschung und -prüfung, Unter den Eichen 87, D-12205 Berlin, Germany*

Received 28 October 1999; received in revised form 14 December 1999; accepted 16 December 1999

Abstract

Conventional simultaneous thermal analysis, capillary-coupled TG–MS, in situ and ex situ Raman and Mössbauer spectroscopy, as well as chemical analysis have been used for the investigation of the first decomposition step of the mixed valence chloroferrate $(dmpipzH_2)_6[Fe(II)Cl_4]_2[Fe(III)Cl_4]_2[Fe(II)Cl_5][Fe(III)Cl_6]$. Under argon at ca. 200°C, an almost complete reduction proceeds in a solid state reaction forming Fe(II). It is accompanied by the release of HCl and, to a minor degree, carbon containing species. A multi-phase product with at least two chloroferrate species, coke, and C,H,N-containing polymers is formed. Binuclear iron complexes, such as $(dmpipzH)_2[Fe(II)_2Cl_6]$, and small amounts of $(dmpipzH)[Fe(III)Cl_4]$ have been proposed to be the major and minor component of the product mixture, respectively.

Keywords: Mixed valence chloroferrate; Thermal decomposition; Intramolecular reduction

1. Introduction

By allowing equimolar aqueous solutions of 1,4-dimethylpiperazine (dmpipz) and iron(II) chloride in 3 M hydrochloric acid to crystallize at room temperature, the presence of atmospheric oxygen leads to partial oxidation of iron. Therefore, one does not obtain the hypothetical $(dmpipzH_2)[Fe(II)Cl_4]$ representing a homologue of the series of 1,4-dimethylpiperazinium halogenometalates, $(dmpipzH_2)[M(II)X_4]$ (M=Co, Zn; X=Cl, Br) [1,2]. Dark brown crystals are formed which are stable in air and contain more chloride than expected. Its crystal structure turned out to be rather unusual, even exciting. Besides the cations in chair form, the structure of $(dmpipzH_2)_6[Fe(II)Cl_4]_2[Fe(III)Cl_4]_2[Fe(II)Cl_5][Fe(III)Cl_6]$ **1** contains six distinct, mononuclear chloroferrate anions arranged on a threefold axis. Tetrahedral, octahedral, and, for the first time with Fe(II), trigonal bipyramidal metal coordinations occur (Fig. 1) [3].

It should be noted that, after separation of the mixed-valence chloroferrate **1**, the final product of the iron oxidation crystallizes from the same solution within several months. The deep red crystals of $(dmpipzH_2)_2[Fe(III)(H_2O)_2Cl_4][Fe(III)Cl_4]Cl_2$ **2** are

* Corresponding author. Fax: +49-30-2093-7392.
E-mail address: feistm@chemie.hu-berlin.de (E. Kemnitz).

0040-6031/00/$ – see front matter
PII: S0040-6031(00)00546-3

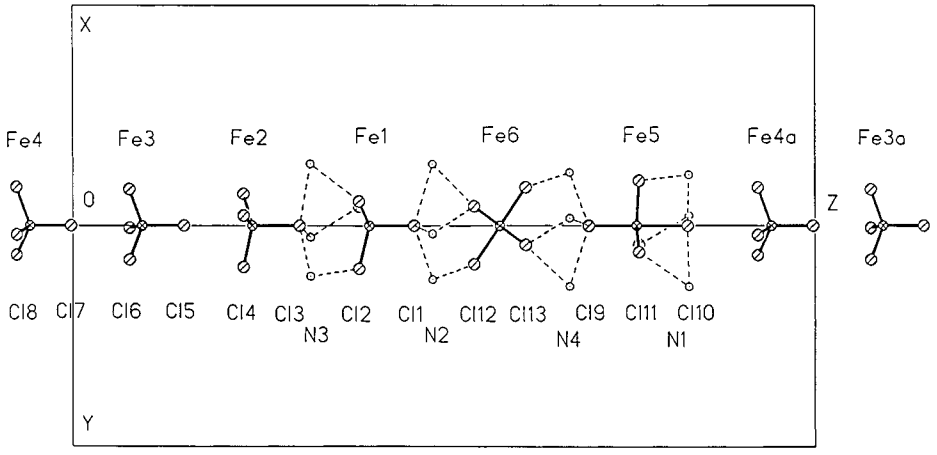

Fig. 1. Arrangement of the Fe–Cl polyhedra on the threefold axis in [0 0 1] direction in the crystal structure of **1** (N···Cl hydrogen bridges — dotted lines; the sequence of the chloroferrate anions is as follows: $[Fe(III)Cl_4]^-$ $[Fe(II)Cl_4]^{2-}$ $[Fe(II)Cl_4]^{2-}$ $[Fe(III)Cl_6]^{3-}$ $[Fe(II)Cl_5]^{3-}[Fe(III)Cl_4]^-$).

also stable in air [4]. Taking into account the remarkable structural features in **1** and the unexpected chemical properties, it was imperative to study the thermally induced changes with various spectroscopic methods.

2. Experimental

2.1. Synthesis and chemical analysis

The title compound **1** can be obtained via two synthetic routes. The first one starts with Fe(II) half of which is slowly oxidized by air to give Fe(III). The second one is the direct synthesis under oxygen-free conditions starting with the molar ratio required for the structure of **1**, i.e. Fe(II):Fe(III)=1:1. All details of the syntheses and the chemical analyses including the redox-titrimetric estimation of Fe(II)/Fe(III) are given in Ref. [3].

2.2. Thermal analysis

Conventional simultaneous thermoanalytical (STA) curves have been recorded in order to understand the thermal phenomena and to yield the appropriate temperatures for the following semi-preparative experiments (300–500 mg) in quartz tubes with flowing argon or air. The samples were heated up to the chosen temperatures with approximately the same heating rate as in the STA run, held at this temperatures for 3–5 min and then cooled down under the gas flow. Thus, sufficient sample quantities have been obtained to process all chemical and spectroscopic investigations necessary for the attribution of the thermal effects. Due to the influence of differing intergranular conditions on the diffusion processes in the solid phase, the interpretation of quantitive data from an STA measurement cannot be applicated a priori to the conditions of separate heating runs in a gas flow tube. For reliable (reciprocal) chemical interpretation, analytical control is required and parallel TG–MS measurements have been undertaken as well. It has been established that the different thermoanalytical equipment yielded rather coincident STA curves and that the heating experiments safely reproduced the mass losses taken from the TG curves.

2.3. Apparatus

NETZSCH-Thermoanalyzer STA 429 with the data acquisition system 414/1; mini sample holder system with the following specifications: Pt/PtRh10 thermoelements, platinum crucibles, sample mass 7–10 mg, α-Al_2O_3 as reference, heating rate 5 K/min, purge gas argon (MESSER-GRIESHEIM Ar 5.0), flow rate 100 ml/min; no further sample pretreatment except grinding in an agate mortar; data evaluation by using

the instrument manufacturer's software SW/STA/531.123_2 without further data treatment; precision of temperature measurement of the sample holder checked regularly by measuring recommended standard substances, e.g. Sn, Li_2SO_4, Al [5,6].

SEIKO TG–DTA-220 coupled with QMG 421 C (BALZERS) via a heated quartz capillary (100°C), sample mass 6–15 mg, purge gas helium, nitrogen or air, flow rate 200 ml/min, heating rate 10 K/min; ion current (IC) intensity measurement for characteristic fragments in the *multiple ion detection mode*(MID) preceded by a *bargraph mode* measurement in a given *m/z* range, e.g. *m/z* 14...120.

2.4. Raman and Mössbauer spectroscopy

All details for the measuring devices and the experimental setup are described in Ref. [3].

3. Results

The rather nonspecific decomposition behaviour of **1** in air is expressed in a discontinuously shaped TG curve without separation of any partial steps that could allow a more detailed investigation. In argon, on the other hand, a well-separated TG step (190–230°C) occurs with a corresponding endothermal effect (T_i=209; T_p=223°C) (Fig. 2). It is then followed by a second endothermal decomposition stage (245–400°C) with more or less separated DTA effects. They cannot be attributed to distinct TG steps indicating hereby a less specific reaction behaviour. Earlier results obtained on chlorocobaltates [7] and -manganates [8] have shown that in this temperature range under inert atmosphere a variety of reactions occurs. Evaporation of dmpipz·HCl and decomposition of the organic base overlap and the complicated redox reactions can yield mixed metal halide phases containing considerable amounts of carbon and nitrogen, e.g. $[MnCl_2{\cdot}(1-x)C_cH_hN_n]$ ($x\approx0.75...0.87$) [8] or even coke. Therefore, our interest was concentrated on the first TG step.

The reactions occurring during the first TG step proceed as solid phase reactions. As stated by visual inspection, only a very slight sintering and a colour change from greenish-brown to black take place. The product is almost X-ray amorphous and the elemental ratio changes from C:H:N:Cl=3:8:1:2.25 to 3:7.3:1:2.

TG–MS measurements in helium (Fig. 3) reproduced the general character of the STA curves in Fig. 2 and lead us to the following four basic statements.

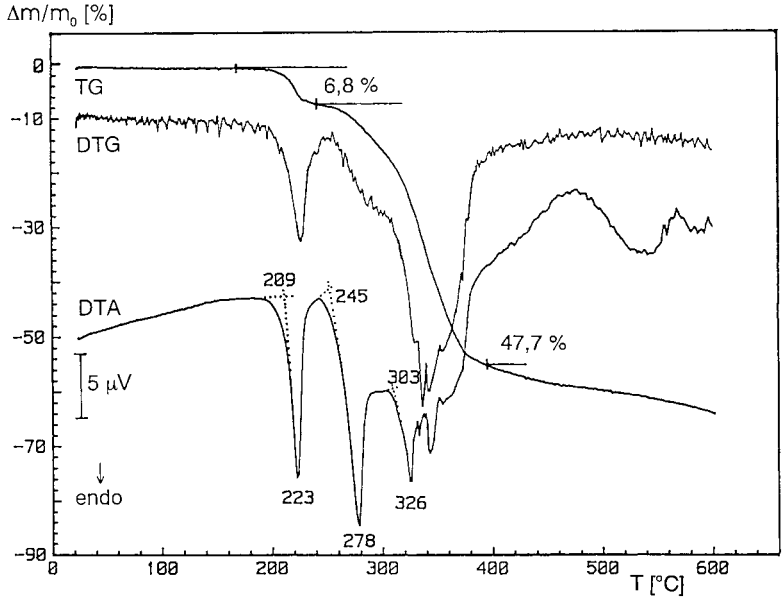

Fig. 2. STA curves of **1** in argon.

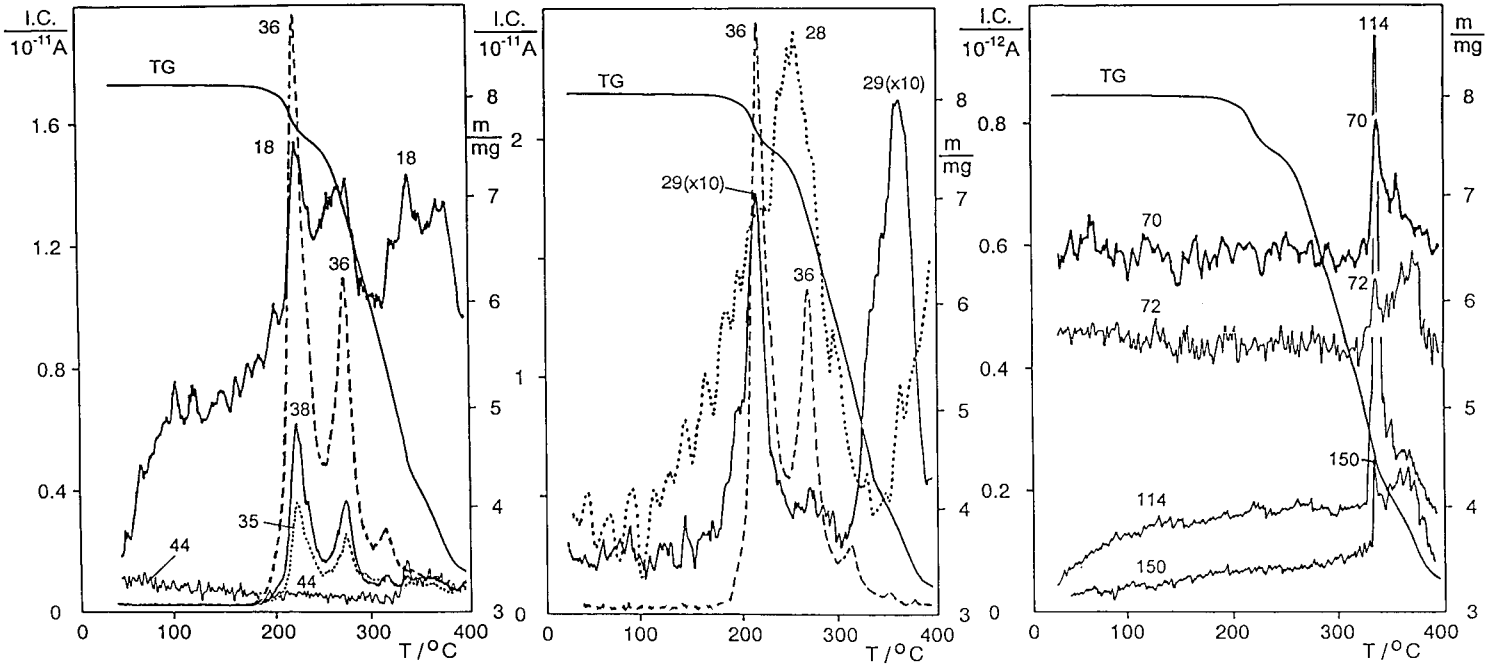

Fig. 3. TG–MS curves of **1** in helium for various IC intensities (The curves for *m*/*z*=70 and 72 are shifted for better legibility).

(a) The small mass loss at ca. 200°C is predominantly caused by the release of HCl (m/z=35, 36, 38) and, to a minor degree, by the release of decomposition fragments of the cation (m/z=29). This agrees with the mentioned change in analytical composition. (b) The completely different shape of the IC curves for m/z=28 and 29 demonstrates that they belong to fragments originating from different sources and that nitrogen is not formed in either the first or the following stages. (c) At higher temperatures, the release of the free base dmpipz (m/z=114) and dmpipz·HCl (m/z=150) occurs.[1] A very small amount of elemental chlorine seems to form (m/z=70, 72) which would be in accordance with earlier findings [8]. (d) The complicated IC curve for m/z=18 with three maxima indicates that the water release is caused by different reasons. The following three reasons have to be considered: water is liberated 'from the depth of the grain' [7,9] as a consequence of the preparation route even if the structure does not contain H_2O molecules and, secondly, it is formed during the redox reactions of the cation degradation ('reaction water'). Thirdly, small quantities of water might be formed via the reaction of OH^- groups, which possibly substitute Cl^- in the chloroferrate anions, with the protons of the organo ammonium cations.

The most surprising observation was obtained by the Mössbauer spectroscopic investigation. In Fig. 4, the variation in the sum spectra of **1** after heating up to 230°C is shown. It proves that nearly complete reduction of Fe(III) has taken place. An estimation of the various contributions to the experimental spectrum by a least squares method (program FAMOS) results in 96.3% Fe(II) and a minor component of 3.7% Fe(III).

The Raman spectroscopic investigation of the residue after heating (Figs. 5–7) yielded the following five basic results: (a) The frequencies attributed to the ions $[Fe(II)Cl_5]^{3-}$ (202 cm^{-1}) and $[Fe(III)Cl_6]^{3-}$ (281 cm^{-1}) [3] disappear. (b) The shoulder at 295 cm^{-1} belonging to $[Fe(II)Cl_4]^{2-}$ becomes more intensive and shifts to higher values. (c) The shoulder of the signal at 330 cm^{-1} nearly disappears. It had

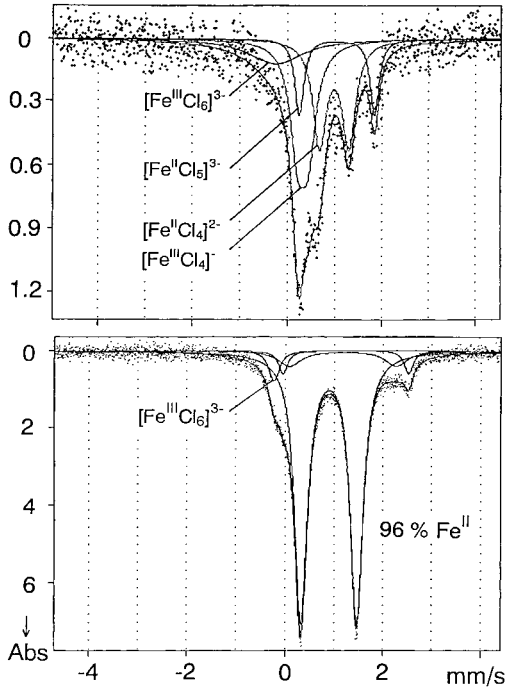

Fig. 4. Comparison of the ^{57}Fe Mössbauer spectra of **1** (above) and of the product obtained after heating to 230°C (below).

been assigned in Ref. [3] to a second crystallographically different $[Fe(III)Cl_4]^-$ ion existing in the structure of **1**. (d) The product does not represent a single phase, but contains at least two chloroferrate species. This is illustrated by Fig. 6 where the different Raman spectra are shown which have been obtained from differently coloured sample sites.[2] (e) The product contains elemental carbon as well. Due to the well-known Raman spectroscopic features of carbon allowing a safe distinction between coke, graphite, and diamond in the frequency range from 1300 up to 1610 cm^{-1} [11] the detection of carbon is unequi vocal but its actual quantity can be small. Fig. 7 demonstrates the evolution of the carbon bands in the Raman spectra for increasing temperatures of sample treatment.

[1] It cannot be excluded that the peaks for the base and the base hydrochloride are shifted to higher temperatures which would be due to a retarding effect of the capillary.

[2] ESR measurements confirmed the formation of a product containing at least two iron species. Due to strong exchange interactions between the nearly neighboured Fe(II) and Fe(III) sites a distinction of the iron valence states was impossible [10].

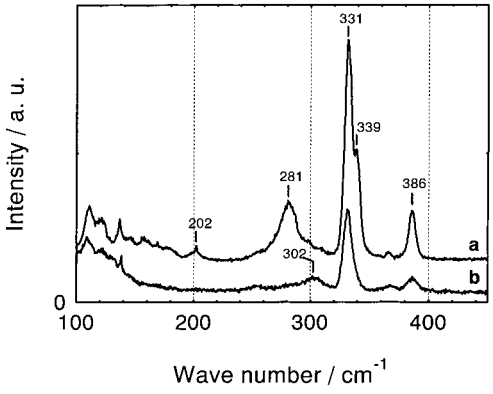

Fig. 5. Raman spectra of **1** (a) and of the product obtained after heating to 230°C (b).

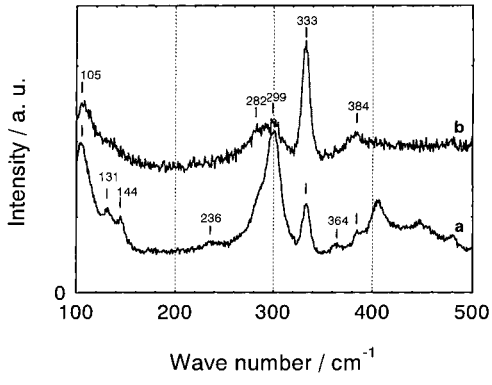

Fig. 6. Raman spectra of pale (a) and darker particles (b) of the heated product.

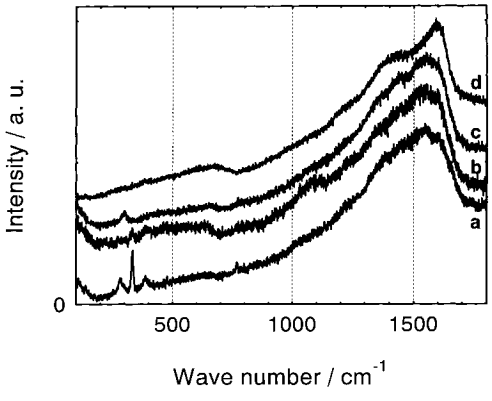

Fig. 7. Raman spectra of the product obtained after heating to 225°C (a); 230°C (b); 290°C (c); 400°C (d). The spectra were normalized to the same maximum intensity.

4. Discussion

The mass loss of 6–9% found in the temperature range 200–230°C which has been safely reproduced in various experiments appeared to correspond to the liberation of either 1 mol dmpipz·HCl (calc. 7.57%) or 3 mol HCl only (calc. 5.50%). But no reasonable interpretation of this first step, e.g. in the form of a chemical equation, could be derived with respect to further results which have been obtained from TG–MS measurements (C-containing fragments, m/z=29, cf. Fig. 3) and from visual inspection as well. For an example, the absence of a white deposit on colder parts of the apparatus was inconsistent with the supposed liberation of dmpipz·HCl. Furthermore, taking into account the properties and stabilities of chloroferrate complexes known, the single one that could have been proposed as a stable product would be the $[Fe(III)Cl_4]^-$ unit. But the obtained quantitative data, e.g. the chloride balance, did not correspond to that idea. However, all these considerations became obsolete with the observation that nearly complete reduction forming Fe(II) had taken place.

The Raman spectroscopic results can be summarized with the disappearance of the more complicated structural units like $[Fe(II)Cl_5]^{3-}$ and $[Fe(III)Cl_6]^{3-}$ favouring the simpler tetrahedral geometry together with the formation of chlorine-bridged units, probably $[Fe(II)_2Cl_6]^{2-}$, which has been mentioned in the literature [12]. This can be derived from an inspection of the relative line intensity changes. This delivers a more reliable information than the absolute line intensities. The changes occur by groups: compared to the valence vibrations between 250 and 400 cm^{-1}, the relative intensity of the deformations around 100 cm^{-1} increases and reaches 1/3 of the line at 330 cm^{-1}(cf. Fig. 5b). This indicates changes in coordination and symmetry. If a higher dimensioned coordination environment is formed, molecule vibrations are hindered due to limited space. Consequently, the valence vibrations decrease whereas the deformations increase. It seems reasonable, therefore, to propose here the formation of bridged chloroferrate species.

This interpretation is in good accordance to the Mössbauer spectroscopic data except for the identification of the minor component as tetra- or hexachloroferrate(III). This might be due to slightly different

Table 1
Mössbauer spectroscopic data (298 K) for **1** after heating to 230°C

Doublet	Attribution	δ (mm s^{-1})	Δ (mm s^{-1})	Γ (mm s^{-1})	Int (%)
1	$[Fe(III)Cl_6]^{3-}$	−0.21	0.08	0.23	3.7
2	$(Fe(II)Cl)_n$	0.91	1.13	0.32	82.9
3	$(Fe(II)Cl)_n$	1.20	2.18	0.57	8.5
4	$(Fe(II)Cl)_n$	1.26	2.57	0.22	4.9

temperatures during the sample preparation for the spectroscopic investigation (overlapping of partial steps). The quadrupole splitting Δ and the isomer shift δ for the Fe(III) component (cf. Table 1) indicate that the minor component is $[Fe(III)Cl_6]^{3-}$ with almost ideal octahedral geometry (Δ=0.08 mm s^{-1}) whereas the Raman data have been interpreted in terms of $[Fe(III)Cl_4]^{-}$. The formed Fe(II) main component, on the other hand, is strongly distorted. The Δ value indicates a symmetry between those for $[Fe(II)Cl_4]^{2-}$ (0.6) and for $[Fe(II)Cl_5]^{3-}$ (1.6 mm s^{-1}) which would be consistent with the idea of the hexachlorodiferrate(II) unit.

It should be noted that the destruction of $[Fe(II)Cl_5]^{3-}$ and $[Fe(III)Cl_6]^{3-}$, which turned out from the Raman data, is related to the liberation of Cl which can then form HCl as a product of hydrogen abstraction from pyrolysis intermediates (cf. Scheme 1). One can presume that the HCl formation does not proceed via an ionic mechanism. Consequently, the electron should remain in the halometalate matrix and could serve as reductant of Fe(III).

Another source of electrons has to be discussed with respect to the organic base cation. Scheme 1 shows a possible reaction via radical cations which explains the formation of electrons acting as reductants and of elemental carbon. It may exist in the form of coke and/or 'irregular polymers', such as known from the Maillard reaction, which contain considerable amounts of C, H, N. Therefore, carbon is the oxidation product whereas iron(III) is reduced. The formal average oxidation state of carbon in the dmpipz molecule is −1.33; therefore, an oxidation producing carbon should easily take place.

5. Conclusions

The variety of chemical and spectroscopic methods applied allows us to describe the first decomposition stage qualitatively by the evolved gases and the phase composition of the residue (Scheme 2) but no quantitative interpretation, e.g. in the form of an correct chemical equation, can be derived for this multitude of reactions.

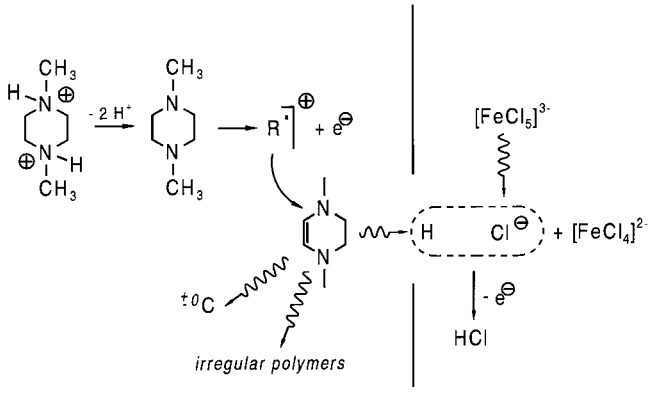

Scheme 1

$$(dmpipzH_2)_6[Fe^{II}Cl_4]_2[Fe^{III}Cl_4]_2[Fe^{II}Cl_5][Fe^{III}Cl_6]$$

$$\downarrow \quad \Delta m \ 6...9\ \%$$

$$(dmpipzH)_2[Fe^{II}{}_2Cl_6] \ , (dmpipzH)[Fe^{III}Cl_4] \ , C \ , \text{polymers}, \ HCl \uparrow$$

Scheme 2

Almost all Fe(III) was reduced resulting in 96% Fe(II) in the product but some Fe(III) always remains which is present as the hexa- or the tetrachloroferrate(III). On the other hand, the chemical analysis proves that all the iron and practically the whole cationic part remains in the solid residue which allows us to presume that a considerable fraction of the cationic frame remains rather unchanged. Therefore, 'intact' chloroferrate complexes in a matrix of monoprotonated cations and anionic complexes may exist. Based on stoichiometry (dmpipz: Fe≈1:1), the cations must be monoprotonated. This agrees with literature information where monoprotonated $(trienH)^+$ species have been reported for solid halogeno complexes [13]. The ratio Fe(II)/Fe(III) in the product as well as in the actual proportion of C,H,N-containing irregular polymers and/or coke depends on a multitude of influencing factors which cannot be separated from each other. A partial overlapping of first and second steps of decomposition resulting in an uncertain temperature profile as well as differing intergranular conditions which influence the diffusion processes have to be taken into account.

References

[1] M. Feist, S. Troyanov, E. Kemnitz, Z. Anorg. Allg. Chem. 621 (1995) 1775.
[2] M. Feist, S. Troyanov, E. Kemnitz, Z. Naturforsch. 51b (1996) 9.
[3] M. Feist, S. Troyanov, H. Mehner, K. Witke, E. Kemnitz, Z. Anorg. Allg. Chem. 625 (1999) 141.
[4] S. Troyanov, M. Feist, E. Kemnitz, Z. Anorg. Allg. Chem 625 (1999) 806.
[5] K. Heide, Dynamische Thermische Analysenmethoden, VEB Deutscher Verlag für Grundstoffindustrie, Leipzig, 1982.
[6] H.K. Cammenga, W. Eysel, E. Gmelin, W. Hemminger, G.W.H. Höhne, S.M. Sarge, Thermochim. Acta 219 (1993) 333.
[7] M. Feist, R. Kunze, D. Neubert, K. Witke, E. Kemnitz, J. Therm. Anal. 49 (1997) 635.
[8] M. Feist, S. Troyanov, A. Stiewe, E. Kemnitz, R. Kunze, Z. Naturforsch. 52b (1997) 1094.
[9] K. Heide, D.-H. Menz, C. Schmidt, L. Kolditz, Z. Anorg. Allg. Chem. 520 (1985) 32.
[10] R. Stösser, G. Scholz, to be published.
[11] V. Huong, Diamond Related Mater. 1 (1991) 33.
[12] B.F.G. Johnson, C.M. Martin, M. Nowotny, W. Palmer, S. Parsons, J. Chem. Soc. Chem. Commun. 1997, 977.
[13] L.M. Vallarino, V.L. Goedken, J.V. Quagliano, Inorg. Chem. 11 (1972) 1466.